ISSN 1063-7788, Physics of Atomic Nuclei, 2026, Vol. 89, Suppl. 2, pp. S218–S225. © Pleiades Publishing, Ltd., 2026.
Russian Text © The Author(s), 2026, published in Voprosy Atomnoi Nauki i Tekhniki, Seriya: Termoyadernyi Sintez, 2026, Vol. 49, No. 1, pp. 41–51.

# Boron Carbide Ceramics as Neutron Shielding for ITER Port Plugs

**A. A. Shoshin[a,b,c,]*, A. V. Burdakov[a,c], M. V. Ivantsivskiy[a], S. V. Polosatkin[a,b,c], Yu. S. Sulyaev[a,b], A. M. Semenov[a,c], D. E. Gavrilenko[a], S. Yu. Taskaev[a,b], D. A. Kasatov[a,b], D. E. Kravtsov[d], N. V. Sorokina[d], A. I. Ovsienko[e], and V. I. Rumyantsev[e]**

[a]*Budker Institute of Nuclear Physics, Siberian Branch, Russian Academy of Sciences, Novosibirsk, 630090 Russia*
[b]*Novosibirsk State University, Novosibirsk, 630090 Russia*
[c]*Novosibirsk State Technical University, Novosibirsk, 630073 Russia*
[d]*ITER Project Center, Moscow, Russia*
[e]*Virial, St. Petersburg, 194156 Russia*
**e-mail: A.A.Shoshin@inp.nsk.su*

Received November 14, 2025; revised February 14, 2026; accepted February 26, 2026

**Abstract**—During the work on integrating the diagnostics into the ITER ports, a problem arose with providing the required radiation protection. It was proposed that a large amount of a neutron-absorbing material, boron carbide, be placed in the vacuum chamber in the port plug. The chemical composition and the thermal and vacuum properties of various $B_4C$ ceramics from several manufacturers were studied. Sintered ceramics in the form of blocks with holes were selected. A specification for the production of ceramics for ITER ports was agreed upon. Experiments on irradiation of ceramics with neutrons at the VITA accelerator were carried out. The degradation of mechanical properties after prolonged fast neutron irradiation was investigated. Serial production of sintered ceramics was started. The ITER Organization has approved the End of Manufacturing reports on the serial batches of ceramics.

**Keywords:** boron carbide, neutron shielding, ITER, outgassing rate, port engineering, port integration

**DOI:** 10.1134/S1063778826140036

## 1. INTRODUCTION

The goals of the ITER diagnostic ports are to house the equipment and ensure its operability, including providing protection of diagnostics from various loads, including neutron ones. Since a port typically contains several different diagnostic and auxiliary systems, usually developed in various countries, the placement of equipment and its protection was named “integration” [1, 2]. An ITER port consists of a port plug, which is under vacuum, port interspace, a biological shield, and a port cell (Fig. 1). The equatorial port plug consists of a structure and three diagnostic shield modules (DSMs) located inside it.

The neutron shield should not only reduce the neutron flux during plasma discharge (which is necessary for the normal operation of various detectors), but also ensure a low level of port activation such that the personnel could work in the port after the discharge has ceased. The main requirements to be demonstrated during port design are as follows: the shutdown dose rate (SDDR) near the port plug must be no more than 100 μSv/h after $10^6$ s (12 days) and no more than 10 μSv/h after 24 h at a distance of 30 cm from the biological shield in the port cell [1, 3] (Fig. 1).

The neutron yield in ITER plasma at a power of 700 MW should be $2.48 \times 10^{20}$ neutr./s at a neutron energy of 14 MeV, which creates a neutron flux of $\sim 10^{14}$ neutr./(cm$^2$ s) on the first wall [4]. The difficulty lies in the fact that both the entire port plug and the individual DSMs included in it have strict design constraints on dry weight: 45 t for the entire equatorial port plug and 10 t for each DSM in it, which does not allow the use of classical iron–water shield of significant thickness [1].

In 2010, the conceptual design review (CDR) of the basic structure of the equatorial port plug was successfully defended. For neutron calculations, the port plug was taken as a solid layered cube made of steel and water, for which the mass was neglected [5]. There were no through holes for diagnostics in it (the real ports will contain cutouts), due to which the neutron calculations showed compliance with the design requirements.

In 2012, neutron calculations were performed for a fairly detailed integrated EPP 1. The port plug con-

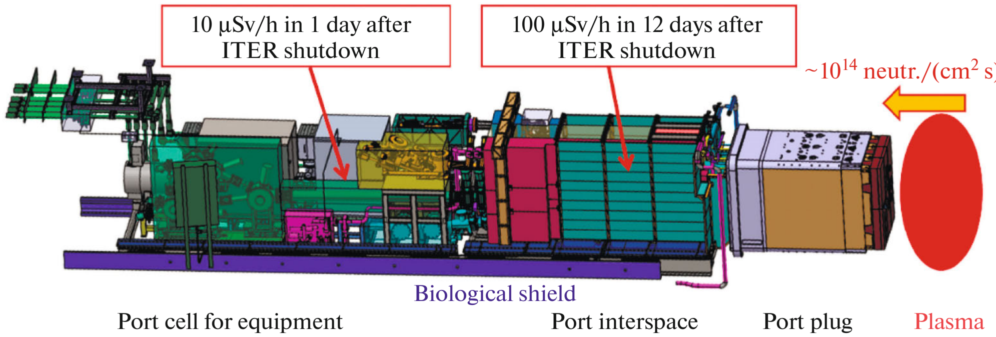


**Fig. 1.** Layout of the ITER equatorial diagnostic port 11 [7], approximate neutron flux on the diagnostic first wall, and dose rate requirements after reactor shutdown in various zones [3]. The port plug is under vacuum; its rear closure plate is the vacuum boundary and the first physical barrier for tritium retention [8, 9].

sisted of only steel and cooling water. For these calculations, the port mass constraint was taken into account, so voids appeared in the port plug. In addition, straight channels for diagnostics from the hot zone to the port interspace were made. The neutron calculations showed that SDDR in the port interspace is two orders of magnitude higher than the requirement of 100 μSv/h [6]. It was immediately suggested that the voids should be filled with a filler possessing low density (due to the weight limitation of the entire port plug) and good ability to slow down and/or absorb neutrons.

When it became clear that the required neutron shielding of the port could not be provided without a filler, it became necessary to select an optimal material. The ITER Organization performed neutron calculations on attenuation of a monoenergetic neutron flux with energies of 1 keV, 1 MeV, and 14 MeV passing through a very simple DSM model with a filler [10]. A large number of materials were compared (Al, Ti, W, Mo metals; steels; boron and tungsten carbides; glasses; ceramics; calcium and zirconium hydroxides; Ti and Zr hydrides; polymers; concretes; and water).

If the filler inside DSM has a fixed mass of 1 t, the best results in terms of the relative efficiency of neutron shielding were shown by polyethylene and borated polyethylene. Using a combustible material with a low melting point near the reactor's hot zone is impossible; therefore, variants with polyethylene were not even discussed.

The next (in the shielding efficiency) DSM was that with 1 t of water inside. Water moderates neutrons well, but using a significant amount of water for port shielding is very complicated because of additional requirements for pressurized cooling water in the ports (it is necessary to ensure a turbulent flow in the baking mode) and the specifics of French legislation (the decree on pressurized nuclear equipment ESPN) [9]; i.e., the requirements of ITER and French legislation [9] do not allow creating a water "pool" inside the DSM that could provide good neutron shielding. A detailed description of French legislation (including the ESPN decree) and ITER Organization requirements as applied to the design and manufacture of ITER components is presented in [9], including the examples of classification of DSMs as pressure equipment in a nuclear facility.

The DSM with boron carbide was the fourth in terms of the relative shielding efficiency at a fixed filler weight, the best variant in this case being that enriched with the $^{10}B$ isotope. However, this variant was rejected because of the extremely high price of $^{10}B$-enriched ceramics.

As a result, in 2014 it was concluded that boron carbide is the best material that can be used in ITER port DSMs, but only if vacuum tests confirm its suitability [10]. The choice of boron carbide is quite understandable: due to its low atomic weight and high neutron capture cross-section, boron carbide is an effective absorber of both fast and slow neutron fluxes. Boron carbide is also chemically inert and thermally stable under the expected operating conditions.

In 2013, the Budker Institute of Nuclear Physics, Siberian Branch, Russian Academy of Sciences (BINP SB RAS); ITER Project Center; and ITER Organization started work on the integration of diagnostic ports (EP-11 [7], UP02, UP08 [11]). The port integrators faced the problem of finding a way to use $B_4C$ and getting an approval on its use, obtaining ceramic samples from manufacturers, performing comprehensive research on them, proving the possibility of using ceramics in ITER diagnostic ports, and obtaining all the required approvals to start the procurement of ceramics.

The first proposal at BINP on the use of boron carbide in EP-11 was to pour boron carbide powder into steel boxes with cutouts for diagnostic systems in the port. A similar proposal was considered in the ITER Organization report [10]; boron carbide is used in the same way in the absorber elements (AEs) of fission reactors.

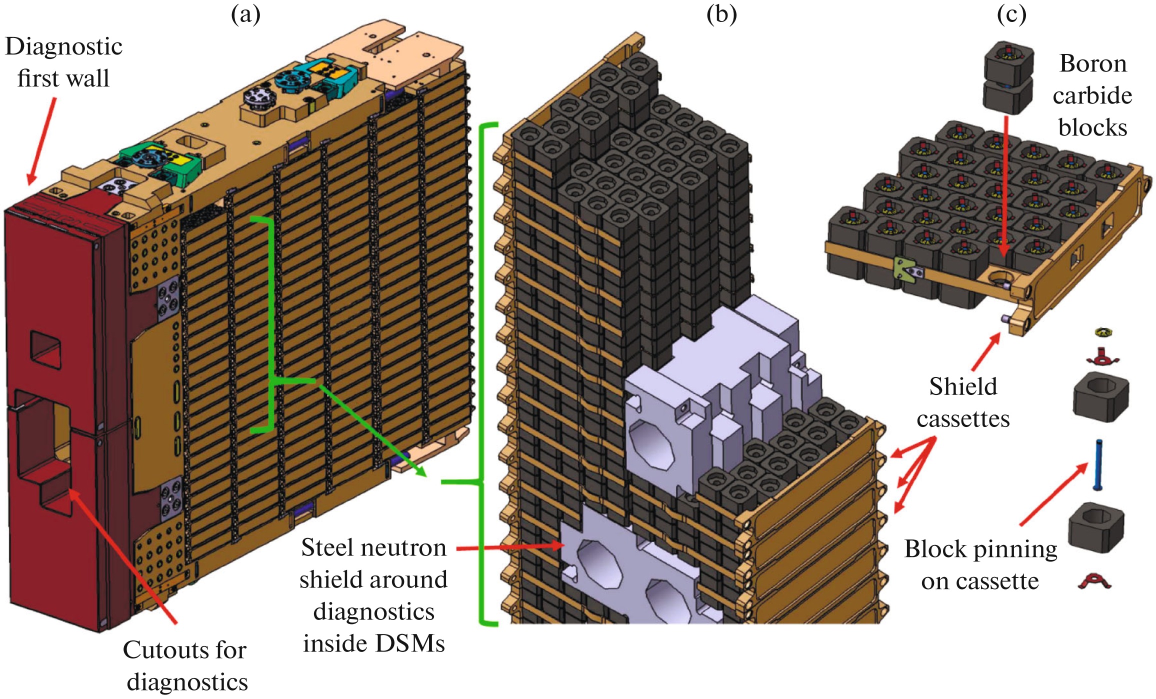


**Fig. 2.** (a) Layout of radiation shield of the diagnostic shield modules (DSMs) using the example of DSM no. 1 of ITER equatorial port 11 (EP-11) (one cassette in the top row is made transparent), (b) part of the second row of shield cassettes and steel shield around diagnostics (some cassettes are made transparent for visualization), (c) shield cassettes with boron carbide ceramic blocks and block fastening.

The proposal to pour boron carbide in the form of pellets into the cutouts of an all-metal DSM frame was made by American colleagues and later by European integrators. In both cases (powder or pellets), two problems arise: providing heat removal from boron carbide heated by neutrons and gamma quanta during the discharge and providing compliance with ITER vacuum requirements. It turned out that in the ITER vacuum chamber, it is strongly not recommended to create trapped volumes [12], so this idea was rejected. Fusion for Energy and IDOM have a special opinion on this issue and continue the integration of European ITER ports using the concept of pouring $B_4C$ pellets into the cavities of a metal frame. With this approach, a problem arises with another ITER requirement, namely, to ensure, in the baking mode, the heating of all elements in the vacuum chamber to a temperature of at least 180°C within two days (clause 4.1.2.6 in [3]). The baking mode is designed for degassing the vacuum chamber before the start of experiments with hot plasma.

After the ban on the use of $B_4C$ powder, BINP proposed using boron carbide ceramics in the form of tiles tightly stacked in steel boxes. This form of ceramic blocks is the cheapest for manufacturing. The use of boron carbide ceramic products (tiles, pellets) as a filler has a number of advantages compared to the use of powdered boron carbide: low specific surface area and porosity, increased density that is close to crystalline, low surface outgassing, shape stability, lower dust formation under thermomechanical loads, and high thermal conductivity.

During the joint development (with the ITER Organization) of a modular design for diagnostic ports, it was proposed that boron carbide-based ceramics be used in the form of blocks with a hole, which are placed on cassettes (trays) (Fig. 2) [1, 7, 13]. The blocks are fixed in the cassettes with steel rods with steel disc springs placed on them (Fig. 2).

At the final design review (FDR) stage of EP-11 in 2020, a DSM model was used for neutron calculations, in which the entire free space is filled with cassettes with boron carbide and steel shielding around the diagnostics (Fig. 2). Additional improvements were made to reduce SDDR, namely, blocks of borated concrete were added into accessible places in the port interspace and port cell, and other improvements were made [14]. Neutron calculations were performed for the SA-2 scenario (20 years of ITER operation in various modes, including discharges with a power of 500 and 700 MW) [15]. The calculations showed that the ITER requirements for the dose rate in the port interspace after reactor shutdown (SDDR) can be met [14]!

**Table 1.** Thermal properties of ceramics according to the ITER_D_457TBH specification [19] and measurement results for sintered ceramics (Virial)

| Properties of ceramics and measurement results | Temperature | | |
|---|---|---|---|
| | 25°C | 100°C | 500°C |
| Specific heat ($C_p$), J kg$^{-1}$ K$^{-1}$, requirements | 900–1050 | 1100–1310 | 1800–2000 |
| Measurement results, ±10% | 1026 | 1308 | 2001 |
| Linear thermal expansion coefficient, $10^{-6}$ K$^{-1}$, requirements | — | 3.10–3.30 | 4.50–4.78 |
| Measurement results, ±5% | — | 3.12 | 4.78 |
| Thermal conductivity, W m$^{-1}$ K$^{-1}$, requirements | 27.0–42.0 | 21.0–30.9 | 15.0–21.0 |
| Measurement results, ±10% | 32.71 | 30.81 | 19.85 |

## 2. STUDIES OF THE CHEMICAL COMPOSITION AND THERMAL PROPERTIES OF VARIOUS BORON CARBIDE CERAMICS

An important problem that had to be resolved was the type of ceramics to be used. The properties and price of boron carbide-based ceramics depend significantly on the manufacturing technology. There are several main types of boron carbide ceramics [16–18]:

(1) *Hot pressing* is performed at high temperatures (2000–2200°C) and pressures. These ceramics are very expensive, and the productivity is low. The density of the ceramics is 2.52 g/cm$^3$, which is very close to the theoretical maximum. The elastic modulus is >450 GPa.

(2) *Reaction bonding* is a relatively inexpensive and high-performance method based on cold (automatic) pressing of blank parts followed by their high-temperature (up to 1500°C) impregnation with molten silicon; the reaction with the latter forms a high-density material. In this case, however, the ceramic contains an appreciable proportion (10–15 wt %) of the silicon impurity (ballast), which lowers the boron content. The density is ~2.64 g/cm$^3$. This is higher than that of hot-pressed ceramics, which is critical for ITER ports with a strict mass limitation. The elasticity modulus is 400 GPa.

(3) *Sintering or pressureless sintering*—cold (automated) pressing and subsequent sintering in a furnace (~2200°C). This method allows the production of ceramics in large quantities and is much cheaper than hot pressing. With this method, possible porosity is ~5%. The density of 2.3–2.4 g/cm$^3$ depends on the production process. The elasticity modulus is ~360 GPa.

Numerous studies were performed to choose suitable boron carbide ceramics and demonstrate compliance of its properties with the ITER Organization requirements [1, 16–18]. The chemical composition of the sintered, hot-pressed, and reaction-bonded ceramics from various manufacturers was investigated. The amount of impurities in sintered and hot-pressed ceramics does not exceed 1%, which meets the ITER requirements. Hot-pressed ceramics has lower porosity, but is much more expensive, and the production rate is very limited. For the ITER ports for which BINP is responsible for integration, sintered ceramics from the Virial company was chosen.

A detailed specification for the manufacture of ceramics, ITER_D_457TBH [19], was agreed upon with the ITER Organization. The specification gives requirements to the chemical composition, thermal and vacuum properties of the ceramics, and quality ensurance requirements for the manufacturer. The requirements to the thermal properties of the ceramics are given in Table 1. Studies are also under way at BINP on the resistance of boron carbide ceramics to pulsed heating [20–22].

The thermal properties of sintered ceramics were investigated, and their compliance with the specification requirements [19] was demonstrated. The measurement results are given in Table 1.

## 3. VACUUM PROPERTIES OF VARIOUS BORON CARBIDE CERAMICS

The conceptual design of the ITER vacuum system did not suggest the use of ceramics in ports. Therefore, during port integration, it was necessary to demonstrate that a large amount of ceramics in the vacuum chamber could still be used for diagnostic port shielding, despite the additional outgassing. It was necessary to demonstrate that the ceramics does not contain hazardous impurities and has good vacuum properties, in particular, that it satisfies all the requirements of the ITER Vacuum Handbook (IVH) [12]. In particular, IVH requires that all materials in the ITER vacuum chamber have a specific outgassing rate below $1 \times 10^{-7}$ Pa m$^3$ s$^{-1}$ m$^{-2}$ for hydrogen and $1 \times 10^{-9}$ Pa m$^3$ s$^{-1}$ m$^{-2}$ for impurities at a temperature of 100°C [12].

A procedure for vacuum testing of ceramics was agreed upon with the ITER Organization, including pre-cleaning, heating the samples in vacuum to 200–240°C for 2 days (which simulates the baking mode conditions in ITER), cooling the samples, repeated heating them to 100°C, and measurements [17, 18].

The first experiments showed that some types of ceramics could satisfy these requirements [16]. The outgassing of $B_4C$ ceramics in vacuum at 100°C has not been measured previously.

Ceramic blocks will fill the whole free space in the diagnostic ports (Fig. 2). In equatorial port 11 alone, more than 40 thousand ceramic blocks with a total surface area of 407 $m^2$ will be located [17, 18]. Because of the large area of ceramics, additional vacuum tests had to be carried out to reliably confirm the possibility of using sintered ceramics [1, 18, 23].

A total of 638 ceramic samples with dimensions of 55 × 55 × 5 mm and a total area of 4.56 $m^2$ were used [1, 18]. The tests showed that after 24 h in vacuum at 100°C, the ceramics meets the requirements of IVH [12] and the first versions of the ceramics manufacturing specification [19]. After 30 months in vacuum, the specific outgassing rate of the ceramics decreased to $2.1 \times 10^{-9}$ Pa $m^3$ $s^{-1}$ $m^{-2}$ [1].

The area of the vacuum chamber was 0.5 $m^2$, i.e., an order of magnitude smaller than the area of the tested ceramics (4.56 $m^2$); accordingly, the gas flow from the samples was three times higher than the background outgassing of the chamber. Thus, the data obtained became the most reliable and accurate among the results of vacuum tests in the ITER Organization's electronic database.

After discussion in the ITER Organization with participation of their vacuum group, it was decided to further tighten the requirements on the outgassing of ceramics in the specification [19]. The new very stringent requirements for ceramics are as follows: outgassing is limited to $1 \times 10^{-8}$ Pa $m^3$ $s^{-1}$ $m^{-2}$ for hydrogen at 100°C and below $1 \times 10^{-10}$ Pa $m^3$ $s^{-1}$ $m^{-2}$ for impurities. The new requirements for ceramics are 10 times more stringent than the requirements for any other material in the ITER vacuum chamber.

The previous tests showed that sintered ceramics manufactured by Virial satisfies the new requirements. The results of vacuum tests with delivered ceramic blocks are presented in Section 5.

## 4. ACTIVATION OF CERAMICS WITH NEUTRONS. DEGRADATION OF MECHANICAL PROPERTIES AFTER NEUTRON IRRADIATION

A VITA accelerator neutron source was proposed and developed at BINP SB RAS for the introduction of the boron-neutron capturing method for therapy of oncological diseases into clinical practice [24–26]; in different modes, the source can generate neutrons of various energies—from cold to fast neutrons. At VITA, experiments were carried out on irradiation of boron carbide ceramic samples with both fast [17] and slow neutrons [18]. Irradiation with slow neutrons made it possible to measure the manganese concentration in

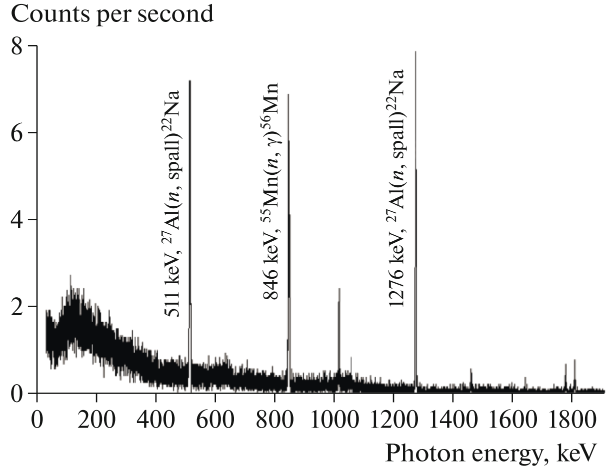


**Fig. 3.** Gamma quantum spectrum of a sintered ceramic sample after irradiation with fast neutrons. For the prominent lines, their energy and the reaction in which gamma quanta were generated are indicated.

ceramics, despite its very low value (0.0001% in sintered ceramics manufactured by Virial Ltd.) and to demonstrate the absence of other activated impurities whose content is regulated by the ITER Organization requirements [18]. The manganese concentration was estimated from comparative irradiation of a series of samples with known contents of this element [18].

Experiments with fast neutrons (average energy 5.68 MeV, fluence $3.6 \times 10^{12}$ n/$cm^2$) made it possible to estimate the activation of ceramics [17]. The dose rate near the ceramic samples was 50 μSv/h immediately after the end of irradiation and only 0.14 μSv/h after 3 days (which is close to the natural background).

The spectrum of gamma quanta emitted by the sample was measured using an SEG-1KP-IFTP spectrometer with a high-purity germanium semiconductor detector. Figure 3 shows the gamma-ray spectrum from sintered boron carbide ceramics measured half an hour after the end of irradiation with fast neutrons [18]. The impurities shown in Fig. 3 have very low contents (for manganese, the content is indicated above), but are easily detected due to the high sensitivity of the method. Thus, the experiments demonstrated that after irradiation with fast neutrons, boron carbide ceramics contains mainly short-lived isotopes, and in a few days after irradiation, the dose rate near the ceramics is very low; i.e., the ceramics should not contribute to the SDDR in the port interspace.

Then, to study the degradation of ceramics under neutron irradiation, an experiment was performed with prolonged irradiation with fast neutrons with a total fluence of $10^{14}$ n/$cm^2$ [25]. After irradiation, none of the samples cracked; the measurements showed that the mechanical strength decreased by 15% (Table 2).

**Table 2.** Degradation of the mechanical properties of sintered boron carbide ceramics (Virial) after irradiation with fast neutrons with a fluence of $10^{14}$ n/cm$^2$

| Physical properties | After irradiation | Initial ceramics |
|---|---|---|
| Density, g/cm$^3$ | 2.14 ± 0.02 | 2.26 ± 0.01 |
| Young's modulus $E$, GPa | 365 ± 14 | 420 ± 7 |
| Bending strength $\sigma_{bnd}$, MPa | 190 ± 13 | 220 ± 11 |

The neutron calculations showed that the typical neutron flux inside the DSM of EP-11 is $10^8$–$10^{11}$ neutrons/(cm$^2$ s) [1, 14], which will give a fluence of $4 \times 10^{11}$–$4 \times 10^{13}$ n/cm$^2$ per shot at a D–T discharge duration of 400 s. Thus, the fluence of $10^{14}$ n/cm$^2$ corresponds to 2–200 ITER D–T discharges depending on the location of the ceramic block inside the DSM of EP-11.

The ITER Organization performed neutron calculations to estimate the amount of helium and tritium that will be produced in the elements of EP-11 during reactor operation [27] (for the SA-2 scenario [15]). The calculations showed that $10^{18}$ helium atoms/cm$^3$ will be produced in the first row of ceramic blocks (that is closest to plasma) [27] and $10^{14}$ atoms/cm$^3$ in the last row [1, 14, 27]. At a boron atom density of $10^{23}$/cm$^3$, the burnup of boron in the experiments at ITER (for the SA-2 scenario [15]) can be considered negligibly small [1].

For optical diagnostics located in the diagnostic ports, the absence of dust is important. Dust can appear due to the cracking of ceramic blocks under the action of the neutron flux. As shown by the experiments conducted at VITA, none of the samples cracked at a fluence of $10^{14}$ n/cm$^2$.

To estimate the swelling of ceramics under neutron irradiation, one can use the published results of boron carbide irradiation in a fast neutron reactor [28]. The swelling coefficient was estimated at 3.5% in [28] at $10^{28}$ neutron captures per 1 m$^3$. As indicated above, the neutron calculations showed that up to $10^{18}$ atoms/cm$^3$ of helium can be formed in the ceramics at the end of the SA-2 scenario [27], due to which the swelling coefficient was estimated at 0.00035%; i.e., it is very small.

## 5. COMMERCIAL PRODUCTION OF $B_4C$ CERAMICS ACCORDING TO ITER ORGANIZATION REQUIREMENTS

The ceramics manufacturing specification [19] requires the manufacturer to prepare a series of documents (Quality Plan, Manufacturing Program, Manufacturing and Control Plan, etc.) and to have them approved by the ITER Organization before the start of production.

The Virial company has started serial production of sintered ceramics for installation in ITER ports. The manufacturer prepared all the documents required by the ITER Organization, which were then approved by the ITER Organization, and successfully passed quality audits.

A cleaning procedure for the manufacturer's ceramic blocks before packaging was also agreed upon in accordance with the ITER Organization requirements: (a) washing the blocks in ethanol; (b) washing in an ultrasonic bath in distillate; (c) annealing in a vacuum furnace at 1000°C for at least 4 h; (d) after annealing and cooling of the furnace, the ceramics are vacuum-packed into individual MET/PE bags (Fig. 4). After this procedure, the ceramics can be removed from the bags without additional cleaning and immediately installed in cassettes for installation in ITER

(a) (b)

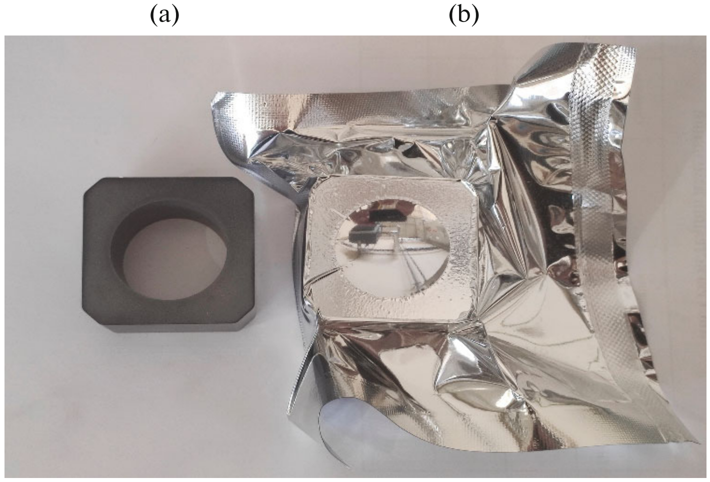

**Fig. 4.** Ceramic block: after the manufacturer's cleaning procedure, each block is placed in a sealed MET-PE bag, and the bag is treated under vacuum: (a) boron carbide ceramic block; (b) the same block in a MET-PE bag.

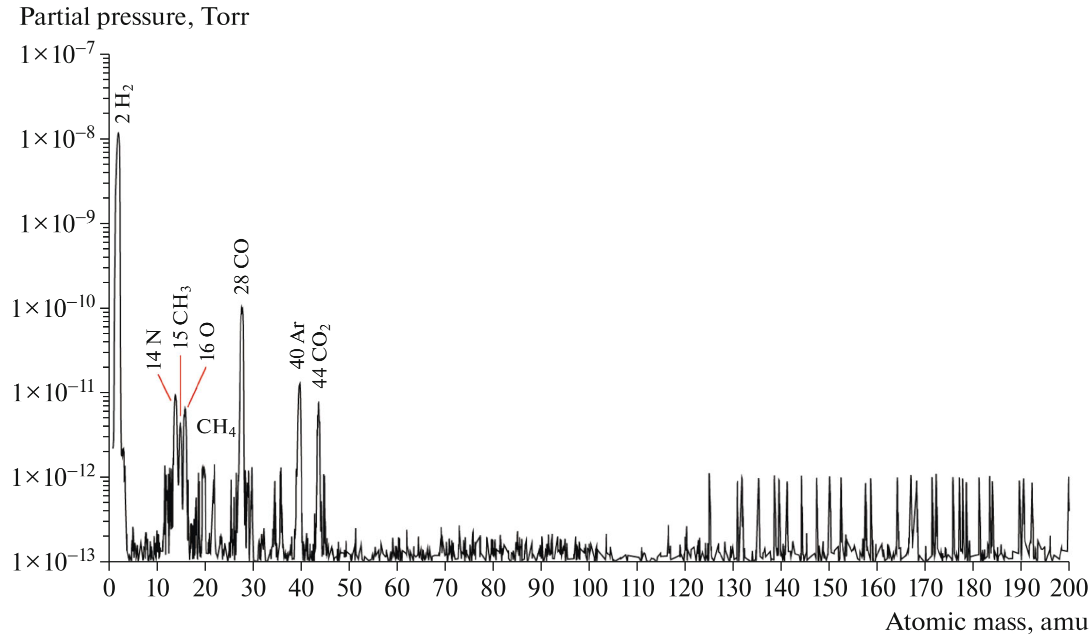


**Fig. 5.** Mass spectrum of gases from the first delivery batch of ceramics manufactured by Virial, measured with a quadrupole mass spectrometer at a sample temperature of 100°C.

ports. The first delivery production batch was vacuum-tested at BINP SB RAS. The measured gas spectrum is shown in Fig. 5. The specific outgassing rate was $8.25 \times 10^{-9}$ Pa $m^3$ $s^{-1}$ $m^{-2}$; the ceramics fully comply with the ITER requirements. The ITER Organization approved the End of Manufacturing report for the first delivery batch [29]. Subsequently, the ITER Organization approved the End of Manufacturing reports for all batches for equatorial port 11 (more than 40 thousand blocks) [30].

## 6. CONCLUSIONS

The chemical composition of boron carbide ceramics and its thermal, vacuum, and mechanical properties have been studied in detail. The long-term studies showed that boron carbide ceramics can be used in the ITER vacuum chamber for neutron shielding of diagnostic ports. The ITER Organization has approved the placement of a large amount of ceramics in the vacuum chamber. Commercial production of sintered ceramic blocks was launched in Russia for diagnostic equatorial port 11 and upper ITER ports 02, 07, and 08. More than 50 thousand ceramic blocks have already been manufactured.

## FUNDING

This work was supported by ongoing institutional funding. No additional grants to carry out or direct thisparticular research were obtained.

## CONFLICT OF INTEREST

The author of this work declares that he has no conflicts of interest.

## REFERENCES

1. A. A. Shoshin, A. V. Burdakov, M. V. Ivantsivskiy, R. Reichle, V. S. Udintsev, J. Guirao, S. Pak, A. Zvonkov, D. Kravtsov, N. Sorokina, Yu. S. Sulyaev, A. Listopad, D. Gavrilenko, A. Taskaev, E. Shabunin, V. Seryomin, S. V. Shiyankov, E. Zaytcev, P. Seleznev, A. M. Semenov, S. Polosatkin, S. Yu. Taskaev, D. Kasatov, I. Shchudlo, M. Bikchurina, V. S. Modestov, A. B. Smirnov, A. A. Pozhilov, A. Lobachev, I. Loginov, O. Shagniev, I. D. Kirienko, and I. Buslakov, Fusion Eng. Des. **178**, 113114 (2022). https://doi.org/10.1016/j.fusengdes.2022.113114
2. J. M. Drevon, M. Walsh, P. Andrew, R. Barnsley, L. Bertalot, M. de Bock, D. Bora, R. Bouhamou, M. F. Direz, A. Encheva, T. Fang, R. Feder, T. Giacomin, M. von Hellermann, S. Jakhar, D. Johnson, Y. Kaschuk, Y. Kusama, H. G. Lee, B. Levesy, D. Loesser, P. Maquet, K. Okayama, R. Reichle, S. Pak, K. M. Patel, C. S. Pitcher, M. Portales, A. P. Arumugam, S. Simrock, V. S. Udintsev, P. Vasu, G. Vayakis, E. Veshchev, C. Walker, C. Watts, and A. Zvonkov, Fusion Eng. Des. **88**, 1306 (2013). https://doi.org/10.1016/j.fusengdes.2013.02.059
3. Project Requirements, (2025). https://user.iter.org/?uid=27ZRW8.
4. M. Loughlin, M. Angelone, P. Batistoni, L. Bertalot, J. Eskhult, Ch. Konno, R. Pampin, A. Polevoi, and E. Polunovskiy, Fusion Eng. Des. **89**, 1865 (2014). https://doi.org/10.1016/j.fusengdes.2014.03.070

5. Diagnostic EPP Neutronics Study CDR, ITER_D_3USYBN (ITER, 2010).
6. S. Salasca, B. Cantone, A. Grosman, B. Esposito, F. Moro, D. Morocco, R. Villari, M. Angelone, E. Rincon, C. Hidalgo, D. Nagy, G. Kocsis, P. Varela, G. Porempovics, G. Perrollaz, K. Patel, Yu. Krivchenkov, and M. Walsh, Fusion Eng. Des. **88**, 602 (2013). https://doi.org/10.1016/j.fusengdes.2013.02.062
7. Yu. S. Sulyaev, E. V. Alexandrov, A. V. Burdakov, M. V. Ivantsivskiy, Yu. N. Zemlyanskiy, K. V. Pischinskiy, S. R. Sharafeeva, S. V. Shiyankov, E. A. Noryshev, A. B. Porotnikov, A. A. Shoshin, A. N. Ivanova, M. V. Klimenko, A. B. Smirnov, A. A. Pozhilov, I. D. Kirienko, and V. S. Modestov, IEEE Trans. Plasma Sci. **48**, 1631 (2020). https://doi.org/10.1109/tps.2020.2985113
8. A. A. Shoshin, Vopr. At. Nauki Tekh., Ser.: Termoyad. Sint. **48**, 105 (2025).
9. A. A. Shoshin, Fusion Eng. Des. **223**, 115550 (2026). https://doi.org/10.1016/j.fusengdes.2025.115550
10. Comparison of materials for neutron shielding for the Diagnostic Shielding Modules, ITER_D_LA8JV5 (ITER, 2014).
11. A. Listopad, E. Alexandrov, A. V. Burdakov, I. Buslakov, A. Gorbovsky, E. Zaitsev, M. V. Ivantsivskiy, I. D. Kirienko, I. Loginov, A. Lobachev, Yu. Manaenkova, V. S. Modestov, P. Seleznev, O. Shagniev, S. V. Shiyankov, and A. A. Shoshin, IEEE Trans. Plasma Sci. **48**, 1721 (2020). https://doi.org/10.1109/tps.2020.2985401
12. ITER Vacuum Handbook, (2019). https://www.iter.org/sites/default/files/media/2024-04/iter_vacuum_handbook.pdf. Accessed March 06, 2026.
13. J. Guirao, M. J. Walsh, V. S. Udintsev, S. Iglesias, T. Giacomin, L. Bertalot, P. Shigin, M. Kochergin, E. Alexandrov, A. Zvonkov, M. V. Ivantsivskiy, T. Fang, Q. Hu, E. Rodríguez, J. Ordieres, R. Juarez, and A. Blanchard, Fusion Eng. Des. **146**, 1548 (2019). https://doi.org/10.1016/j.fusengdes.2019.02.126
14. ITER Neutronics Report, Demonstration of the ALARA Implementation in EP#11, ITER_D_Y86VFC (ITER, 2020).
15. Recommendation on Plasma scenarios, ITER_D_2V3V8G (ITER, 2009).
16. A. A. Shoshin, A. V. Burdakov, M. V. Ivantsivskiy, M. Klimenko, S. Polosatkin, and A. M. Semenov, Fusion Eng. Des. **146**, 2007 (2019). https://doi.org/10.1016/j.fusengdes.2019.03.088
17. A. A. Shoshin, A. V. Burdakov, M. V. Ivantsivskiy, S. Polosatkin, M. Klimenko, A. M. Semenov, S. Yu. Taskaev, D. Kasatov, I. Shchudlo, A. Makarov, and N. Davydov, IEEE Trans. Plasma Sci. **48**, 1474 (2020). https://doi.org/10.1109/tps.2019.2937605
18. A. A. Shoshin, A. V. Burdakov, M. V. Ivantsivskiy, S. Polosatkin, A. M. Semenov, Yu. S. Sulyaev, E. Zaitsev, P. Polozova, S. Yu. Taskaev, D. Kasatov, I. Shchudlo, and M. Bikchurina, Fusion Eng. Des. **168**, 112426 (2021). https://doi.org/10.1016/j.fusengdes.2021.112426
19. 55.QB—Material Specification for the supply of Boron Carbide ($B_4C$), ITER_D_457TBH (ITER, 2025), Vol. 1.3.
20. A. A. Shoshin, A. V. Burdakov, and I. V. Kandaurov, Phys. At. Nucl. **87**, S70 (2024). https://doi.org/10.1134/S1063778824130118
21. D. E. Cherepanov, L. N. Vyacheslavov, V. A. Popov, G. A. Ryzhkov, A. A. Kasatov, A. A. Vasilyev, A. S. Arakcheev, A. A. Ruktuev, I. V. Kandaurov, and A. A. Shoshin, Nucl. Mater. Energy **36**, 101495 (2023). https://doi.org/10.1016/j.nme.2023.101495
22. D. E. Cherepanov, A. V. Burdakov, L. N. Vyacheslavov, S. R. Kazantsev, I. V. Kandaurov, A. A. Kasatov, A. V. Krasilnikov, V. A. Popov, G. A. Ryzhkov, and A. A. Shoshin, Phys. At. Nucl. **87**, S99 (2024). https://doi.org/10.1134/S1063778824130039
23. A. V. Burdakov, A. V. Varand, A. A. Krasnov, O. I. Meshkov, M. A. Mikhailenko, A. M. Semenov, B. P. Tolochko, and A. A. Shoshin, Instrum. Exp. Tech. **65**, 519 (2022). https://doi.org/10.1134/s0020441222030137
24. S. Yu. Taskaev, E. Berendeev, M. Bikchurina, T. Bykov, D. Kasatov, I. Kolesnikov, A. Koshkarev, A. Makarov, G. Ostreinov, V. Porosev, S. Savinov, I. Shchudlo, E. Sokolova, I. Sorokin, T. Sycheva, and G. Verkhovod, Biology **10**, 350 (2021). https://doi.org/10.3390/biology10050350
25. Ya. Kolesnikov, M. Bikchurina, T. Bykov, D. Kasatov, N. Singatulina, I. Shchudlo, E. Sokolova, V. Bobrovnikov, S. Gromilov, A. Sukhikh, et al., Nucl. Instrum. Methods Phys. Res., Sect. B **571**, 165968 (2026). https://doi.org/10.1016/j.nimb.2025.165968
26. S. Yu. Taskaev, *Accelerator Neutron Source VITA* (Fizmatlit, Moscow, 2024) [in Russian].
27. Determination of quantities in EP#11 during machine operation, ITER_D_Y86WVS (ITER, 2020).
28. T. Maruyama, Sh. Onose, T. Kaito, and H. Horiuchi, J. Nucl. Sci. Technol. **34**, 1006 (1997). https://doi.org/10.1080/18811248.1997.9733777
29. EMR $B_4C$ batch 01, ITER_D_DAGDG6 (ITER, 2025).
30. $B_4C$ — Conformity of Material (CoM), ITER_D_CHQRU5 (ITER, 2025).

**Publisher's Note.** Pleiades Publishing remains neutral with regard to jurisdictional claims in published maps and institutional affiliations.
AI tools may have been used in the translation or editing of this article.